

Monopole-Antimonopole Annihilation in a Nematic Liquid Crystal

Andrew Pargellis,⁽¹⁾ Neil Turok,⁽²⁾ and Bernard Yurke⁽¹⁾

⁽¹⁾*AT&T Bell Laboratories, Murray Hill, New Jersey 07974*

⁽²⁾*Joseph Henry Laboratories, Princeton University, Princeton, New Jersey 08544*

(Received 25 March 1991)

We study the process of monopole-antimonopole (hedgehog-antihedgehog) annihilation in nematic liquid crystals theoretically and experimentally. We show, using a “mini-max” argument, that there exists a stable scaling solution to the nematodynamic equations describing this phenomenon, and find the solution numerically. We study the process experimentally in the uniaxial nematic, 4-cyano-4'-n-pentylbiphenyl, following a pressure jump or thermal quench. We confirm, over 3 orders of magnitude in time, the scaling-solution prediction for the pair separation D . We find $D \propto (t_0 - t)^\alpha$, with $\alpha = 0.5 \pm 0.03$.

PACS numbers: 61.30.Jf, 64.70.Md, 98.80.Cq

Liquid crystals provide a laboratory system in which the dynamics of topological defects produced in symmetry-breaking phase transitions can be explored. Such defects play an increasingly central role in condensed matter, particle physics, and cosmology. It is likely that understanding gained in the study of defect dynamics in liquid crystals will have broad application in other fields. Recently we have shown [1,2] that string defects in liquid crystals [3] are formed in accordance with the Kibble mechanism widely invoked in the cosmological context [4]. The string density scales as t^{-1} in agreement with the predictions of a “one-scale” model analogous to that used for cosmic strings [5,6].

In this paper we explore the dynamics of the point defects (known as “hedgehogs” or “point singularities” in the liquid-crystal literature, or “global monopoles” in the cosmological literature), in particular monopole-antimonopole ($m\bar{m}$) pair annihilation [7]. We are interested in the behavior of free poles in bulk medium—in related experiments, Lavrentovich and Rozhkov [8] and Rapini, Leger, and Martinet [9] considered the annihilation of “boojums” (surface defects in the form of half monopoles), with results similar to those reported here.

A naive model of $m\bar{m}$ annihilation is to argue that the force of attraction between the pair is constant (the energy scaling as the separation D), but the damping force is proportional to the “size” of the m, \bar{m} , given by D . Thus one obtains $dD/dt \propto -1/D$ with solution $D \propto (t_0 - t)^{1/2}$. We shall see how this behavior actually emerges from the field equations. In the simplest “one-constant” approximation, and in the absence of fluid flow, the “nematodynamic” equations [10] describing the relaxation of the liquid-crystal director in the nematic phase are given by

$$\gamma \frac{\partial n^a}{\partial t} = K [\nabla^2 n^a + (\nabla n^b) \cdot (\nabla n^b) n^a], \quad (1)$$

where $n^a(t, \mathbf{x})$ is the three-component director field, constrained to have unit length, and repeated indices are summed. K is the elastic constant and γ a damping constant. Equation (1) is the nonrelativistic analog of the nonlinear sigma model which determines the evolution of global defects produced in cosmology [11].

Scaling solutions occur in partial differential equations when the solution loses dependence on the initial condi-

tions. In our case, as the $m\bar{m}$ separation shrinks to zero, we expect the solution to lose dependence on the details of the long-wavelength modes making up the initial configuration. In this case, dimensional analysis dictates that n^a can depend only on the dimensionless scaling variable $\mathbf{z} = (\gamma/K)^{1/2} \mathbf{x} / (t_0 - t)^{1/2}$, where t_0 is the annihilation time. Then (1) becomes

$$\frac{1}{2} \mathbf{z} \cdot \nabla_{\mathbf{z}} n^a = \nabla_{\mathbf{z}}^2 n^a + (\nabla_{\mathbf{z}} n^b) \cdot (\nabla_{\mathbf{z}} n^b) n^a. \quad (2)$$

This equation follows from the stationarity of the following positive-definite energy functional:

$$\mathcal{E} = \int d^3z e^{-z^2/4} (\nabla_{\mathbf{z}} n^a) \cdot (\nabla_{\mathbf{z}} n^a), \quad (3)$$

where one imposes the constraint $n^a n^a = 1$ with a Lagrange multiplier.

Now we shall argue that a stationary point of (3) actually exists. Consider the set of all possible monopole-antimonopole configurations where the poles are located on the z axis at $z = \pm R$. For each R there exists a configuration that minimizes \mathcal{E} . For $R \ll 1$ the exponential in (3) can be ignored: Then the simple scaling argument of Derrick [12] shows that $\mathcal{E}_{\min} \propto R$. For $R \gg 1$ it is clear that \mathcal{E}_{\min} falls as $e^{-R^2/4}$ since n^a may be taken to be uniform out to a radius of order R . Thus \mathcal{E}_{\min} goes to zero at small or large R . In fact R parametrizes a one-parameter noncontractible loop in configuration space, as long as we identify the $R=0$ “vacuum” with that at $R=\infty$. This is made rigorous by using periodic boundary conditions. One can now imagine deforming this loop to the minimal-energy trajectory through configuration space. A maximum-energy point must occur on this sequence of minimal-energy configurations, corresponding to a stationary point of \mathcal{E} . This corresponds to a classical solution with a single unstable mode. Note also that the argument is quite general in character: In [2] we apply essentially the same argument to show the existence of scaling solutions for string-loop collapse, and for vortex-antivortex annihilation in the two-dimensional XY model.

Such a “mini-max” argument, which may be viewed as an application of Morse theory to infinite-dimensional configuration space, was used by Taubes to rigorously prove the existence of a static monopole-antimonopole solution to the Yang-Mills-Higgs equations [13]. Man-

ton then applied an analogous argument to the standard electroweak theory [14], which led to the construction of the “sphaleron,” an unstable classical solution which plays a central role in electroweak baryon-number violation, a topic of much recent interest. We have not attempted a rigorous proof of the existence of the solution in our case, but have instead used (3) as the basis for an explicit numerical solution.

Before explaining this, let us interpret the unstable mode. It corresponds to a change of scale:

$$\delta n^a(\mathbf{z}) = n^a((1 + \epsilon)\mathbf{z}) - n^a(\mathbf{z}) \approx \epsilon \mathbf{z} \cdot \nabla_{\mathbf{z}} n^a. \quad (4)$$

However, $\mathbf{z} \cdot \nabla_{\mathbf{z}} n^a$ is directly proportional to $\partial n^a / \partial t$, so the perturbation (4) corresponds to a shift in time, and thus a shift in t_0 , the annihilation time. From the time-translation invariance of (1) it is clear that if a single scaling solution exists, there must be an infinite family related by time shifts. What appears as an instability in the coordinates t, \mathbf{z} is merely a shift in the final collapse time t_0 . This may also be seen in the model equation $dD/dt = -1/D$, with scaling solution $D = \sqrt{2}(t_0 - t)^{1/2}$. In terms of $z = D/(t_0 - t)^{1/2}$ and t , one sees the same “instability” of the scaling solution, $z = \sqrt{2}$. Apart from this mode, we expect the scaling solution to be stable to small perturbations, and this is confirmed by our numerical study.

We used (3) as the basis for a numerical “relaxation” procedure. We assume cylindrical symmetry, with the following ansatz for the Cartesian components of \mathbf{n} :

$$\mathbf{n}(\mathbf{z}) = n^\rho \cos(\phi) \hat{\mathbf{e}}_x + n^\rho \sin(\phi) \hat{\mathbf{e}}_y + n^z \hat{\mathbf{e}}_z. \quad (5)$$

As initial conditions we take $n^\rho = \cos(\theta - \bar{\theta})$, $n^z = \sin(\theta - \bar{\theta})$, where $\theta, \bar{\theta}$ are the polar angles from origins located at the m, \bar{m} , respectively. Upon integrating over ϕ , the azimuthal angle, and discretizing, \mathcal{E} becomes a simple function of the (n^z, n^ρ) at each lattice site. Minimization of \mathcal{E} with respect to the director at each site results in replacing the director at that site with a weighted average of the director at neighboring sites. One then sweeps through the lattice minimizing \mathcal{E} at each site in turn. The boundary conditions, at radius $\rho = R$ and $z = \pm Z$ are as follows. We use fixed boundary conditions, with the director perpendicular to the radial boundary, as in the experimental setup below. This means that there has to be an “escaped” +1 string running down the center of the cylinder, which is observed. On the $z = \pm Z$ surfaces we choose the director to take the form of the exact minimal-energy +1 string:

$$\mathbf{n} = \sin[\theta(\rho)] \cos\phi \hat{\mathbf{e}}_x + \sin[\theta(\rho)] \sin\phi \hat{\mathbf{e}}_y + \cos[\theta(\rho)] \hat{\mathbf{e}}_z,$$

with ϕ the azimuthal angle and $\theta(\rho) = 2 \tan^{-1}(\rho/R)$. Cylindrical symmetry dictates that the director $(n^z, n^\rho) = (\pm 1, 0)$ on the z axis.

We could proceed by fixing the director around the poles and then relaxing to $\mathcal{E}_{\min}(d)$ for each d . However, fixing the director near the monopoles is artificial, and actually results in “singular” configurations: The flux tends to collapse onto the z axis, either between the monopoles

or off to $z = \pm \infty$. Instead it is better to replace the exponential $e^{-z^2/4}$ by $e^{-z^2/4L^2}$ and adjust L to keep the poles stationary. By changing coordinates to $\mathbf{z}' = \mathbf{z}/L$, this is seen to be equivalent to changing the scale of the solution (and therefore d) by a factor L .

With this procedure the director is allowed to freely adjust itself everywhere. For small L , as expected we observe the $m\bar{m}$ pair move apart, and for large L they move together, this being preceded by the “flux lines” moving out towards $z = \pm \infty$ before the pair moves apart, or moving in towards the origin before the pair pulls together. By adjusting L to keep the monopoles at fixed separation, one finds a critical scale L_C . The method appears stable and convergent. The end result after 5000 steps is shown in Fig. 1, corresponding to a separation d of 21 grid units, and with $L_C = 12.5$. This corresponds to a scaling solution with $m\bar{m}$ separation

$$D = (d/L_C)(t_0 - t)^{1/2} (K/\gamma)^{1/2} \approx 1.7(t_0 - t)^{1/2} (K/\gamma)^{1/2}.$$

Apart from the one unstable mode we have already accounted for, the scaling solution appears stable, in line with expectation from the mini-max argument.

We now turn to the experiment. In nematic liquid crystals with cylindrical boundary conditions, $m\bar{m}$ pairs have been observed before [15]. The director is forced to

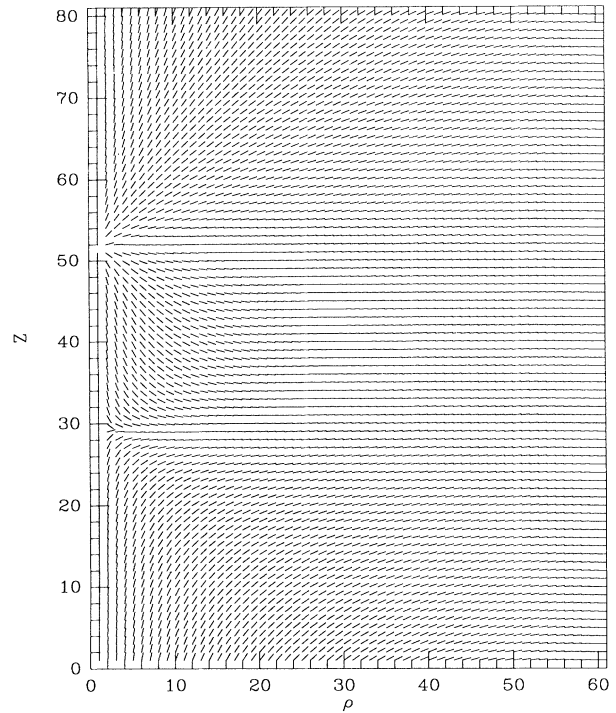


FIG. 1. Result of numerical “relaxation” calculation of the scaling solution for the annihilation of a monopole-anti-monopole pair. The configuration of the director field \mathbf{n} is shown at each site on the 60×80 lattice. Cylindrical symmetry has been used: The full three-dimensional configuration is obtained by a rigid rotation of this plane about the z axis. The poles are located at $z = 30$ and $z = 51$, on the z axis. The boundary conditions are described in the text.

be radial near the capillary walls when they are treated with a homeotropic alignment material, and the director is observed to “escape” along the axis [15–18], forming a diffuse type-1 singularity, even for capillaries down to $0.2\ \mu\text{m}$ in radius [18]. We have studied monopole-antimonopole annihilation in this situation. A similar process was studied in [8] and [9], namely, the annihilation of boojums (half monopoles attached to a surface) in thin films of nematic liquid crystal. Their results for the scaling of the separation of the boojum-antiboojum pair are quite similar to ours for the monopole-antimonopole pair.

Our experiments used the uniaxial nematic 4-cyano-4'-*n*-pentylbiphenyl, known as K15. The isotropic-to-nematic transition occurs at 35.3°C and atmospheric pressure. The apparatus consisted of a quartz capillary, with $0.35 \pm 0.03\text{-mm}$ internal diameter, filled with the K15 liquid crystal. The capillary was treated with a homeotropic alignment material, *N,N*-dimethyl-*N*-octadecyl-3-aminopropyltrimethoxysilylchloride (DMOAP), imposing the boundary condition mentioned above, and then placed between two planar glass windows, with the intermediate region filled with glycerol as an index-matching medium. The cell was mounted on the stage of a transmission optical microscope. Visual images were recorded with an HSV-400 (NAC, Inc.) video recorder at a rate of 200 frames/s.

Various defects, strings ($\pm \frac{1}{2}$ and ± 1 disclinations) and monopoles (hedgehogs), were generated during rapid transitions from the isotropic to the nematic phase. The transition was induced either through rapid pressure jumps or temperature quenches. In the former case, the glycerol bath was heated and the temperature monitored with a type-*K* thermocouple. One end of the capillary was sealed off and the other end was connected to a reservoir, filled with FC-72 (3M, “Fluorinert”), that could be pressurized to 5000 psi. The pressure was increased in less than 50 ms to about 1500 psi, at 36°C , and kept constant. For temperature quenches, the isotropic phase was obtained by heating the capillary to about 40°C . It was then cooled in a glycerol bath at 20°C . A separate study showed the temperature dropped from 40 to 22°C in less than 10 s. After this cooling, the $m\bar{m}$ separation D was observed and measured with time.

Figure 2 shows a typical $m\bar{m}$ annihilation event, spanning 100 s. The $m\bar{m}$ pair, produced in a thermal quench, consists of two monopoles diametrically opposite on what appears as a bright “looplike” optical pattern, oriented along the axis of a capillary of 0.35-mm internal diameter. By rotating the capillary azimuthally one sees that the loops are cylindrically symmetric, so the director configuration is actually ellipsoidal in form. The loop shape is elongated when the $m\bar{m}$ separation distance is comparable to or larger than the capillary radius. Presumably the tension of the type-1 disclination is the driving force making the loop contract. We have always observed loops positioned on the capillary axis to collapse asymmetrically. One pole remains fixed and the other

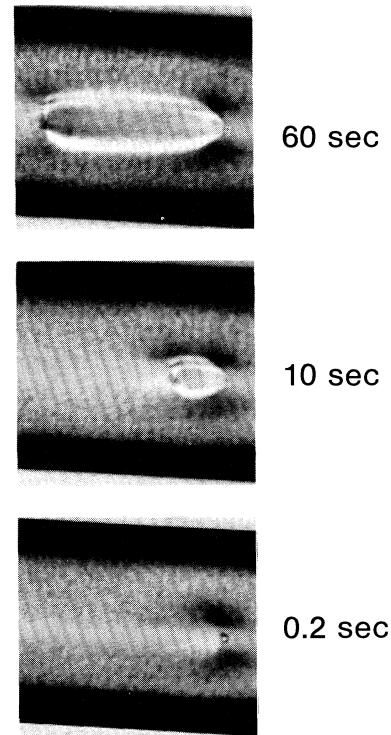


FIG. 2. Sequence showing the collapse of a type-1 disclination loop with a monopole-antimonopole pair on it. Each image is labeled with the time in seconds before the final annihilation. The interpole distance D is about $0.4\ \text{mm}$ in the first image.

moves toward it. This may be due to the preferred direction established by the director configuration escaping along the capillary axis. In the case where the loop was near the capillary wall, both poles approached each other. We also observed an event most analogous to the numerical scaling solution discussed above, where the poles were located on a “linear” type-1 disclination. In this case both poles moved, but one still moved more than the other. Understanding this behavior probably requires going beyond the one-constant approximation.

Figure 3 is a plot of the $m\bar{m}$ separation for several sets of data. All data are from the annihilation of monopoles on loops except the data represented by the crosses, which are for the collapse of monopoles on a linear type-1 disclination, situated along the capillary’s axis. This latter situation occurred only rarely, but as mentioned is the case best represented in the numerical simulation performed above.

The lower data sets were produced with thermal quenches, in a capillary of 0.35-mm inner diameter. The solid squares are for the collapse sequence shown in Fig. 2. The upper data sets, displaced one decade for clarity, were produced with pressure jumps. The open circles are the data for a 0.35-mm capillary, and a pressure jump of 7.6 MPa (1100 psi) at a temperature of 36°C . The other two sets used a capillary of 1.1-mm inner diameter, and a

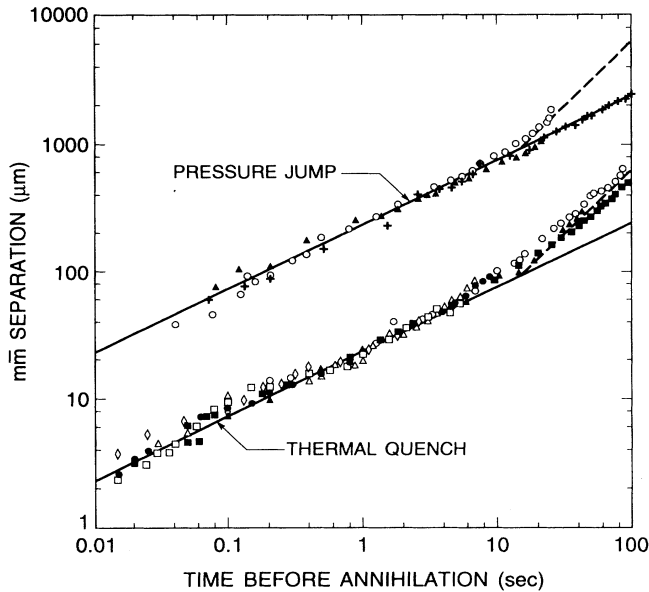


FIG. 3. The intermonopole distance D vs time before the $m\bar{m}$ annihilation time t_0 for several sets of data. The phase transitions were induced by either a thermal quench (lower set of data points) or by pressure jumps (upper set of data points, displaced upwards one decade for clarity). The solid and dashed lines represent the scaling $D \propto (t_0 - t)^\alpha$ with $\alpha = 0.5$ and 1.0 , respectively.

pressure jump of 8.6 MPa at 36.4 °C. Fitting our data by the scaling solution gives $\gamma/K \approx 2.8t/d^2 \approx 5.3 \text{ ms}\mu\text{m}^{-2}$. This is comparable to the value measured directly by Wu and Cox [19], who obtained $\gamma_1/K_{11} \approx 10.5 \text{ ms}\mu\text{m}^{-2}$, by measuring the electro-optic response time.

For all data sets, the $m\bar{m}$ separation scales at late times approximately as $D \propto (t_0 - t)^{0.5}$. In the smaller capillary, for $m\bar{m}$ separations greater than the capillary's inner radius, the scaling is instead given by $D \propto t_0 - t$. The naive argument given above indicates that the damping force on the poles should be independent of D in this case, since the capillary provides a cutoff to the monopole size, but the force should still be constant. This results in D scaling linearly with time, as observed. Similar scaling for the boojum-antiboojum pair separation was observed in [8] and [9] in thin nematic films between two surfaces—one with the pair on it, and the other homeotropically aligned. They found that $D \propto (t_0 - t)^{0.5}$ for thick films and $D \propto t_0 - t$ for thin films. Figure 3 indicates that the results are only weakly dependent on the geometry or the means of generating the defect tangle. It also indicates

that the ratio of the elastic constant to the damping constant is approximately the same for the different temperature and pressure values chosen in the experiment.

N.T. acknowledges the support of NSF Contract No. PHY80-19754 and the support of the Alfred P. Sloan Foundation.

-
- [1] I. Chuang, R. Durrer, N. Turok, and B. Yurke, *Science* **251**, 1336 (1991); I. Chuang, N. Turok, and B. Yurke, *Phys. Rev. Lett.* **66**, 2472 (1991).
 - [2] I. Chuang, A. Pargellis, N. Turok, and B. Yurke, Princeton University Report No. PUP-TH-1249, 1991 (to be published).
 - [3] See, for example, M. Kleman, *Points, Lines and Walls in Liquid Crystals, Magnetic Systems and Various Disordered Media* (Wiley, Chichester, 1983).
 - [4] T. W. B. Kibble, *J. Phys. A* **9**, 1387 (1976).
 - [5] T. W. B. Kibble, *Nucl. Phys.* **B252**, 227 (1985).
 - [6] A. Albrecht and N. Turok, *Phys. Rev. D* **40**, 973 (1989).
 - [7] A simple "monopole" configuration is one where the "director field" \mathbf{n} points radially outward from a singular point. A complication in the case of a nematic liquid crystal is that \mathbf{n} is equivalent to $-\mathbf{n}$, the molecules being invariant under inversion. Naively, this would make a monopole and antimonopole equivalent. However, the *relative* topological charge of two poles is well defined, as discussed in G. E. Volovik and V. P. Mineev, *Zh. Eksp. Teor. Fiz.* **72**, 2256 (1977) [*Sov. Phys. JETP* **45**, 1186 (1977)], and P. Goddard and D. Olive, *Rep. Prog. Phys.* **41**, 1357 (1978), for example.
 - [8] O. D. Lavrentovich and S. S. Rozhkov, *Pis'ma Zh. Eksp. Teor. Fiz.* **47**, 210 (1988) [*JETP Lett.* **47**, 254 (1988)].
 - [9] A. Rapini, L. Leger, and A. Martinet, *J. Phys. (Paris)*, *Colloq.* **36**, C1-189 (1989).
 - [10] P. G. de Gennes, *The Physics of Liquid Crystals* (Clarendon, Oxford, 1974).
 - [11] N. Turok, *Phys. Rev. Lett.* **63**, 2625 (1989); N. Turok and D. Spergel, *Phys. Rev. Lett.* **66**, 3093 (1991).
 - [12] G. H. Derrick, *J. Math. Phys.* **5**, 1252 (1964).
 - [13] C. H. Taubes, *Commun. Math. Phys.* **86**, 257 (1982); **86**, 299 (1982).
 - [14] N. S. Manton, *Phys. Rev. D* **28**, 2019 (1983).
 - [15] C. Williams, P. Pieranski, and P. E. Cladis, *Phys. Rev. Lett.* **29**, 90 (1972).
 - [16] P. E. Cladis and M. Kleman, *J. Phys. (Paris)* **33**, 591 (1972).
 - [17] C. E. Williams, P. E. Cladis, and M. Kleman, *Mol. Cryst. Liq. Cryst.* **21**, 355 (1973).
 - [18] G. P. Crawford *et al.*, *Phys. Rev. A* **43**, 835 (1991).
 - [19] S.-T. Wu and R. J. Cox, *J. Appl. Phys.* **64**, 821 (1988).

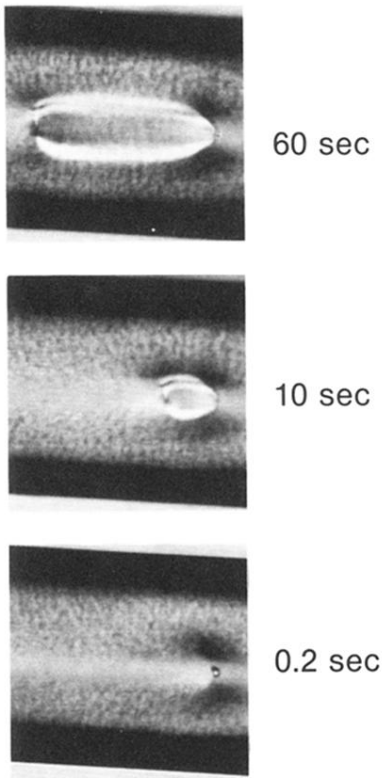


FIG. 2. Sequence showing the collapse of a type-I disclination loop with a monopole-antimonopole pair on it. Each image is labeled with the time in seconds before the final annihilation. The interpole distance D is about 0.4 mm in the first image.